

EURISOL-DS Multi-MW Target Comparative Neutronic Performance of the Baseline Configuration vs. the Hg-Jet Option

Adonai Herrera-Martínez, Yacine Kadi

AB Dept. ATB/EET
European Organization for Nuclear Research (CERN)
CH-1211 Geneva 23, Switzerland

Abstract

This technical report summarises the comparative study between several design options for the Multi-MW target station performed within Task #2 of the European Isotope Separation On-Line Radioactive Ion Beam Facility Design Study (EURISOL DS) [1].

Previous analyses were carried out, using the Monte Carlo code FLUKA [2], to determine optimal values for relevant parameters in the target design [3] and to analyse a preliminary Multi-MW target assembly configuration [4]. The second report showed that the aimed fission rates, i.e. $\sim 10^{15}$ fissions/s, could be achieved with such a configuration. Nevertheless, a preliminary study of the target assembly integration [5] suggested reducing some of the dimensions. Moreover, the yields of specific isotopes have yet to be assessed and compared to other target configurations.

This note presents a detailed comparison of the baseline configuration and the Hg-jet option, in terms of primary and neutron distribution, power densities and fission product yields. A scaled-down version of the baseline configuration (i.e. reduced radius and length), is proposed and compared with the other designs.

The results confirm the feasibility of the reduced target configuration, while obtaining fission product yields comparable to those of the Hg-jet layout, without the technical problems of the latter. Significant fission rates may be obtained with 4 MW of beam power and few one-litre UnatC₃ targets. Moreover, the energy deposited in the liquid metal may be evacuated with reasonable flow rates.

Table of Contents

| | |
|--|----|
| INTRODUCTION..... | 3 |
| PRIMARY PROTON DISTRIBUTION..... | 3 |
| NEUTRON FLUX DISTRIBUTION..... | 5 |
| POWER DENSITIES | 8 |
| FISSION DISTRIBUTIONS AND ISOTOPIC YIELDS..... | 10 |
| INTEGRATION OF THE ASSEMBLIES | 14 |
| CONCLUSIONS..... | 14 |
| ACKNOWLEDGEMENTS | 15 |
| REFERENCES..... | 15 |

Introduction

A thorough study of a preliminary Multi-MW target configuration, optimised for maximum neutron production and complete proton beam containment inside the Hg target, is presented in [4]. In these calculations, large fission rates ($\sim 10^{15}$ fissions/s) were obtained with reasonable fission target volumes, i.e. one to five litres of UnatC₃, in a technically feasible configuration.

Nevertheless, concerns about specific isotope production rates, which are not only proportional to fission rates but also affected by neutron energy, suggested an in-depth comparison of the aforementioned preliminary design with the option of a 2 cm radius Hg jet (Figure 1.a), where the fission target is closer to the neutron source and the neutron energy spectrum is much harder.

Moreover, possible problems in the integration of the Multi-MW target assembly for the preliminary configuration motivated a reduction in the radius of the proton-to-neutron converter, from 15 cm to 8 cm, as presented in Figure 1.b, reducing the Hg target mass from ~ 500 down to ~ 100 kg.

These three options are herein systematically compared, following the methodology and approach previously applied in [3] and [4]. In addition, preliminary values for some fission fragment production rates are given, since this is the ultimate decision parameter for the facility.

Primary Proton Distribution

Based on the reference parameters obtained in the preliminary study of the liquid metal proton-to-neutron converter [1], the target length was set to 46 cm, since this is the proton range in Hg for 1 GeV protons. Thus, the primary shower is almost fully contained inside the Hg target, for the baseline configuration [4].

Conversely, the Hg jet option presents a large amount of primary proton escapes, i.e. $\sim 25\%$ of the proton beam and up to $\sim 10^{13}$ primaries/cm²/s/MW of beam primary flux (Figure 2.a). These large high-energy proton escapes would certainly require a beam dump, and does not seem to take full advantage of the high-power proton beam.

In the case of the scaled-down version of the baseline configuration (Figure 2.b), most of the beam is contained within the target assembly, with primary escapes three orders of magnitude lower than those of the Hg jet option.

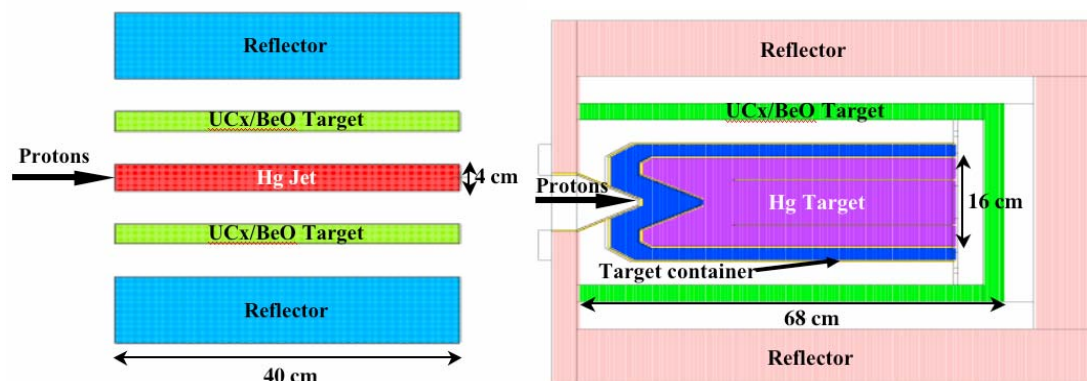


Figure 1. Schematic view of the Hg-jet option, where several elements of the facility have been included, as reported in [6]. Schematic view of the scaled-down baseline configuration, showing different elements of the assembly.

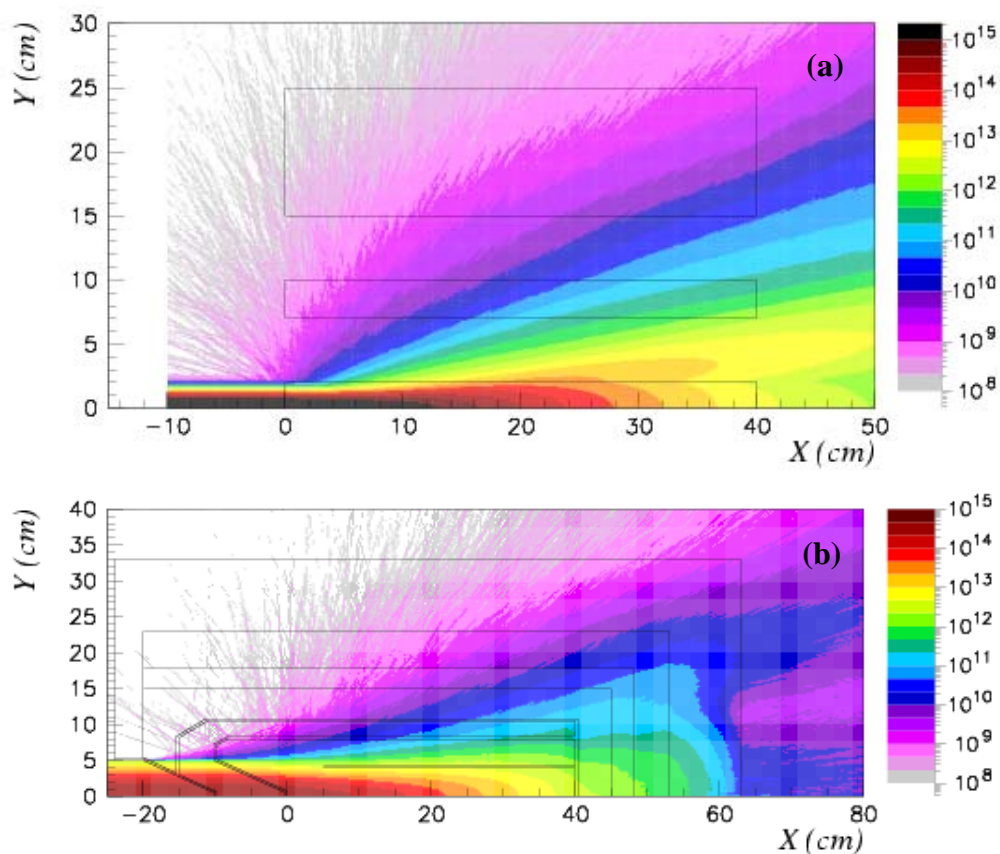


Figure 2. Primary proton flux distribution (primaries/cm²/s/MW of beam) in (a) Hg-jet option and (b) scaled-down version.

Neutron Flux Distribution

All three Multi-MW target options present significant neutron fluxes in the fission target. For the baseline configuration, the neutron flux reaches $\sim 10^{14}$ neutrons/cm²/s/MW of beam (Figure 4.a), similar to those found in nuclear reactors. The scaled-down version presents a higher (twice the average neutron flux) and a more homogeneous distribution in the radial fission target (Figure 4.c) due to the reduced amount of Hg, hence of moderation. In both cases, most of the neutrons are contained inside the assembly and escapes are one order of magnitude lower than the flux in the target.

These escapes could be further reduced by increasing the reflector thickness, or used for other research activities typical of white neutron sources, e.g. time-of-flight cross-section measurements neutron scattering experiments etc. For the Hg jet design, the neutron flux is four times higher in the fission target and presents a more anisotropic distribution, with important neutron escapes both in the front cap (backscattering problems, such as the activation of the beam line) and end cap, as illustrated in Figure 4.b.

In terms of neutron energy spectra, the flux exiting the Hg jet has a peak energy between 1 and 2 MeV and is significantly harder than in the other two cases, where the peak energies are 300 keV and 700 keV for the baseline configuration and its scaled-down version, respectively (Figure 3.a). A harder neutron spectrum presents important advantages for inducing fission in ²³⁸U, since fission probability in this isotope is negligible below the MeV energy range (Figure 3.b).

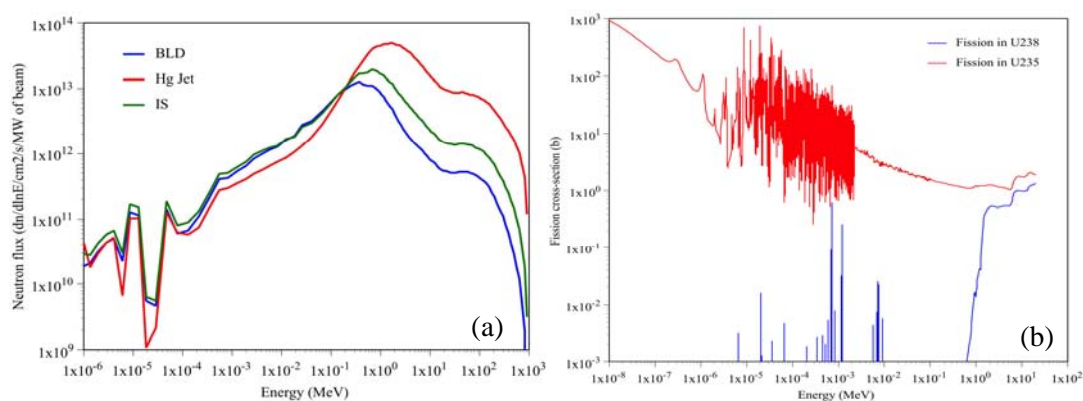


Figure 3. Neutron energy spectra ($dn/dlnE/cm^2/s/MW$ of beam) for the three different Multi-MW target configuration (a), and fission cross-section comparison for ²³⁵U and ²³⁸U (b).

Nevertheless, the large high-energy component (above 50 MeV, and up to 1 GeV) of the neutron flux has a negative impact in terms of radioprotection (displaced neutron

source) and structural damage (deteriorating mechanical properties). This is clearly shown in Figure 5, where very small fluxes escape the reflector in both, the baseline configuration and its scaled-down version, compared to those streaming from the Hg jet design, at least one order of magnitude higher.

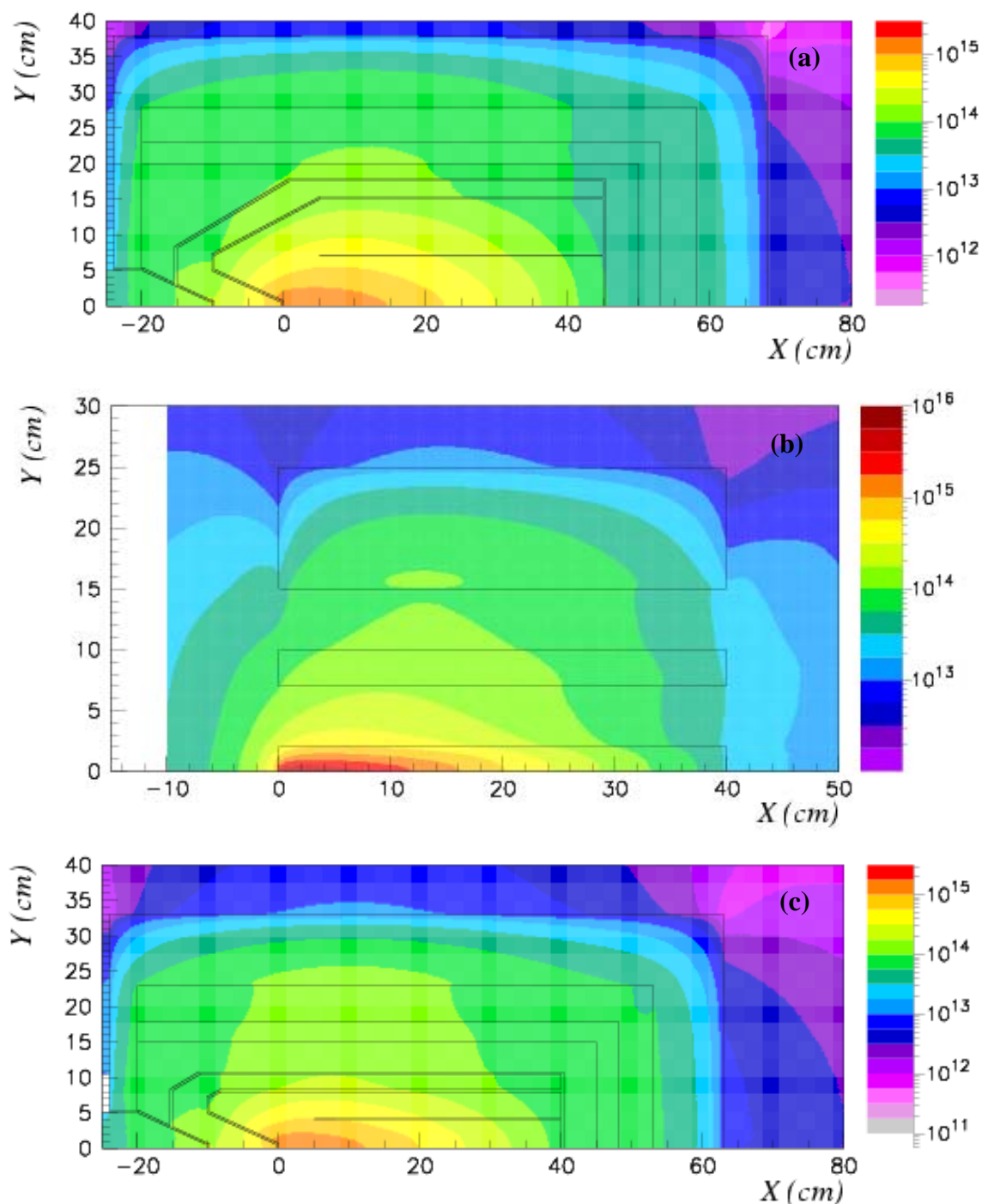


Figure 4. Neutron flux distribution (neutrons/cm²/s/MW of beam) in (a) baseline configuration, (b) Hg-jet option and (c) scaled-down version.

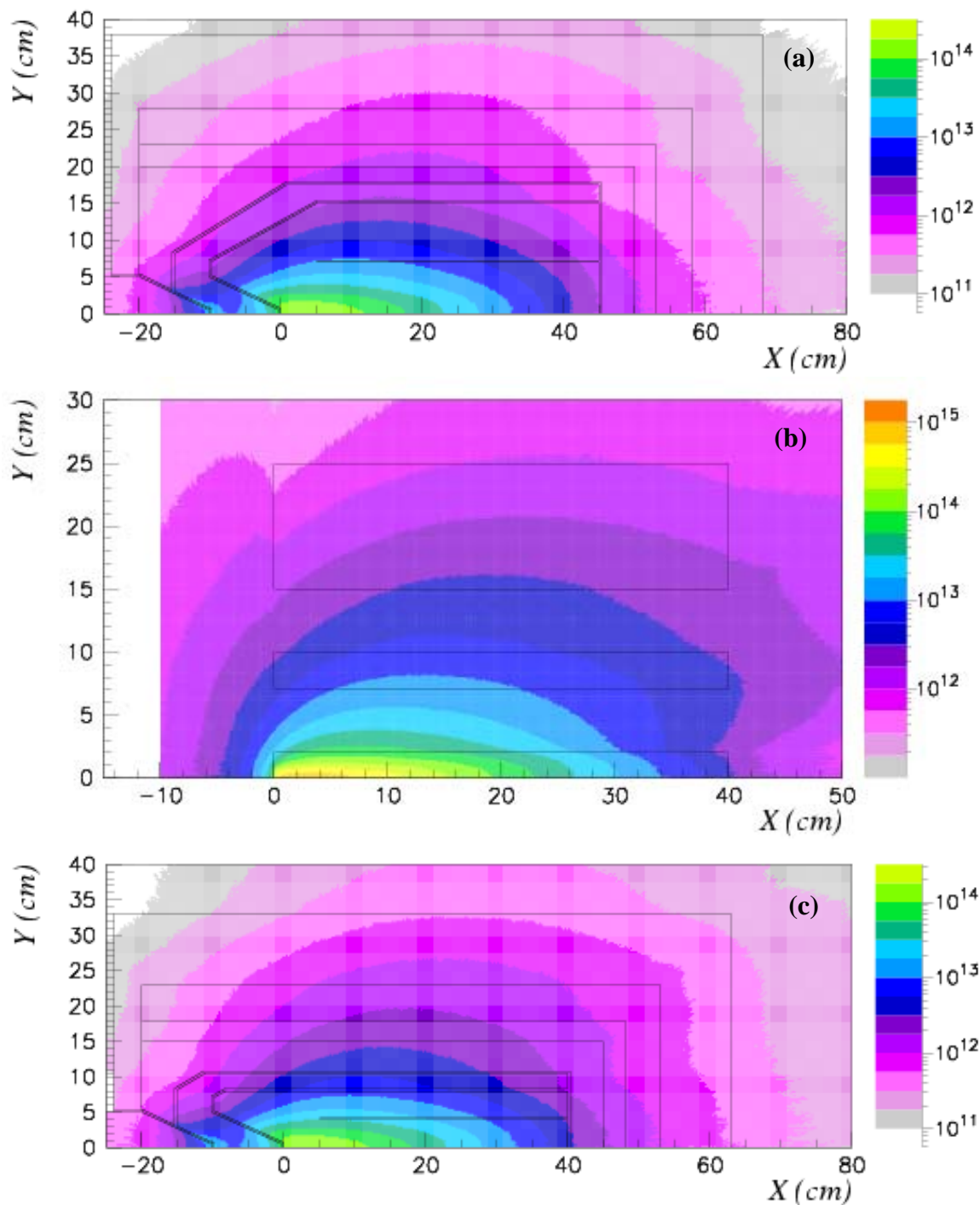


Figure 5. High-energy (above 20 MeV) neutron flux distribution (neutrons/cm²/s per MW of beam) in (a) baseline configuration, (b) Hg-jet option and (c) scaled-down version.

Power Densities

For 1 GeV protons, most of the energy deposition occurs in the first 10 cm beyond the interaction point. The maximum is $\sim 2 \text{ kW/cm}^3/\text{MW}$ of beam for the baseline configuration as well as for its scaled-down version, and lies at $\sim 2 \text{ cm}$ from the interaction point, as shown by Figure 6.a, where the curves displaying the power densities along the beam axis in both configurations overlap. These power densities are technically challenging due to Hg boiling, as illustrated in Figure 6.b. These challenges may be overcome with reasonable flow rates by pressurising the Hg container and using the design detailed in [7].

The energy deposition in the beam window may be another source of problems due to thermally-induced stresses. The maximum power density of $\sim 1 \text{ kW/cm}^3/\text{MW}$ of beam in the window suggests the need of a specific cooling method for this item and a careful choice of material.

Conversely, power densities in the Hg jet design soar to $\sim 22 \text{ kW/cm}^3/\text{MW}$ of beam, requiring very large Hg flows to avoid vaporisation. In free surface jet, the disintegration of the jet [8] due to shock waves from thermal expansion should also be studied and avoided since may pose a myriad of problems, from proton beam loss to structural damage by Hg droplets, cavitation etc.

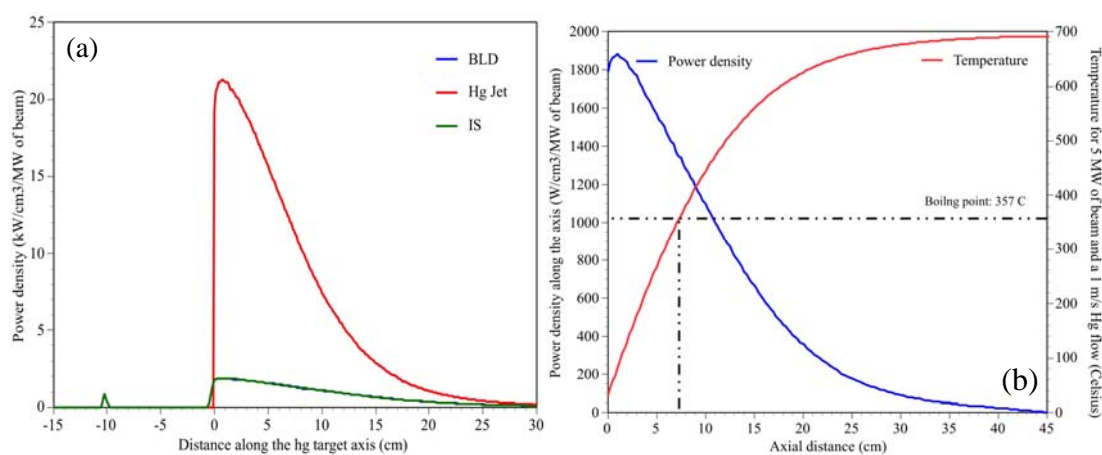


Figure 6. Power density distribution ($\text{kW/cm}^3/\text{MW}$ of beam) for the three Multi-MW target configurations studied (a), and power density distribution and temperature increase along the beam axis for the baseline configuration and its scaled-down version.

In the case of the baseline configuration, 70% of the beam power is deposited in the Hg target (2.8 MW out of the 4 MW of beam, most of it concentrated along the length of the Hg target and extending 5 cm in radius). The scaled-down version absorbs 61% of the beam (2.4 MW). On the other hand, the Hg jet only absorbs 39% of the beam

(1.4 MW), the rest is deposited in the nearby structures, namely the fission target and downstream structures (reflector, shields, front-end parts, etc...).

Figures 7.a and b. also show the energy distribution in the fission target. The baseline configuration and scale-down version present a homogeneous distribution averaging ~ 3 and ~ 5 $\text{W}/\text{cm}^3/\text{MW}$ of beam, respectively. On the other hand, the Hg jet option presents an anisotropic power distribution, ranging from 3 – 20 $\text{W}/\text{cm}^3/\text{MW}$ of beam. This lack of homogeneity may induce temperature differences inside the fission target, which in turn may hinder the diffusion/effusion processes of fission products and generate thermal stresses. In all three configurations, the energy deposition in the UCx target are mostly due to fissions, since they follow the same pattern as those, as can be inferred by comparing Figures 7 and 8.

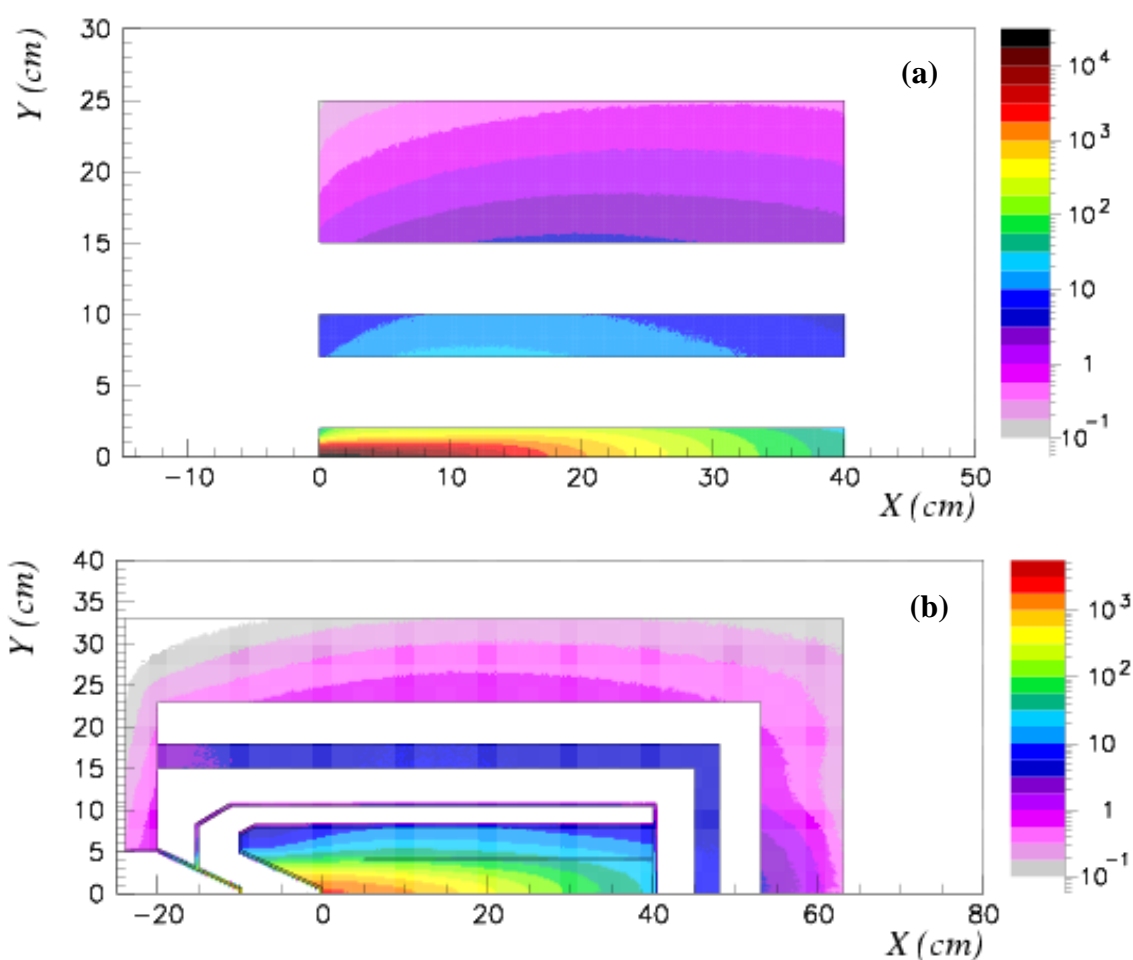


Figure 7. Power density distribution ($\text{W}/\text{cm}^3/\text{MW}$ of beam) in (a) Hg-jet option and (b) scaled-down version.

Fission Distributions and Isotopic Yields

The power densities in the fission target previously presented follow, in fact, the fission density distribution, since the energy released there is mostly due to fissions. Therefore, for the baseline configuration (BLD) and its scaled-down version (IS), the fission density is homogeneous, averaging $\sim 10^{11}$ fissions/cm³/s/MW of beam for the first (Figure 8.a, 10% of which are produced by neutrons above 20 MeV) and $\sim 2 \times 10^{11}$ fissions/cm³/s/MW of beam for the second (Figure 8.c, 20% of which are produced by neutrons above 20 MeV). On the contrary, the Hg-jet option presents a higher fission density ($\sim 4 \times 10^{11}$ fissions/cm³/s/MW of beam, 40% of which are produced by neutrons above 20 MeV) but anisotropically distributed, as illustrated in Figure 8.b and correlated with the previously mentioned power density.

The impact of the reflector may be observed in both, the baseline and its scale-down version, by the increase in fission densities on the outer layer of the fission target. This effect is due to fissions in ²³⁵U from neutrons scattered back by the BeO reflector. On the other and, it does not seem relevant in the case of the Hg jet, where most of the fissions occur where the high-energy neutron flux is largest.

The harder neutron spectrum reaching the fission target in the Hg-jet option has a direct impact on the number of symmetric fissions in the UCx target. Figure 9.a and 9.b show the isotopic distribution of fission products for the three target configurations under comparison. The isotopic yield in this region (produced by high-energy fissions) is one order of magnitude higher in the Hg jet option compared to the baseline configuration ($\sim 4 \times 10^9$ vs $\sim 3 \times 10^8$ isotopes/cm³/s/MW of beam, in Figure 9.b). The scaled-down version presents an intermediate performance, producing $\sim 8 \times 10^8$ isotopes/cm³/s/MW of beam (notice the logarithmic scale).

In terms of asymmetric fissions, originated by lower energy neutrons, differences are not as acute (Hg jet producing three times and twice more fissions than the baseline configuration and its scaled-down version, respectively).

Evaporation and multiple fragmentation products are also more abundant in the Hg jet option due to the streaming of high-energy neutrons and protons into the fission target. This fact may have a negative effect on the fission fragment extraction due to the production of isobars. Indeed, the isotopes generated by direct reactions tend to be proton-rich whereas those originated from fission are neutron-rich, having similar masses.

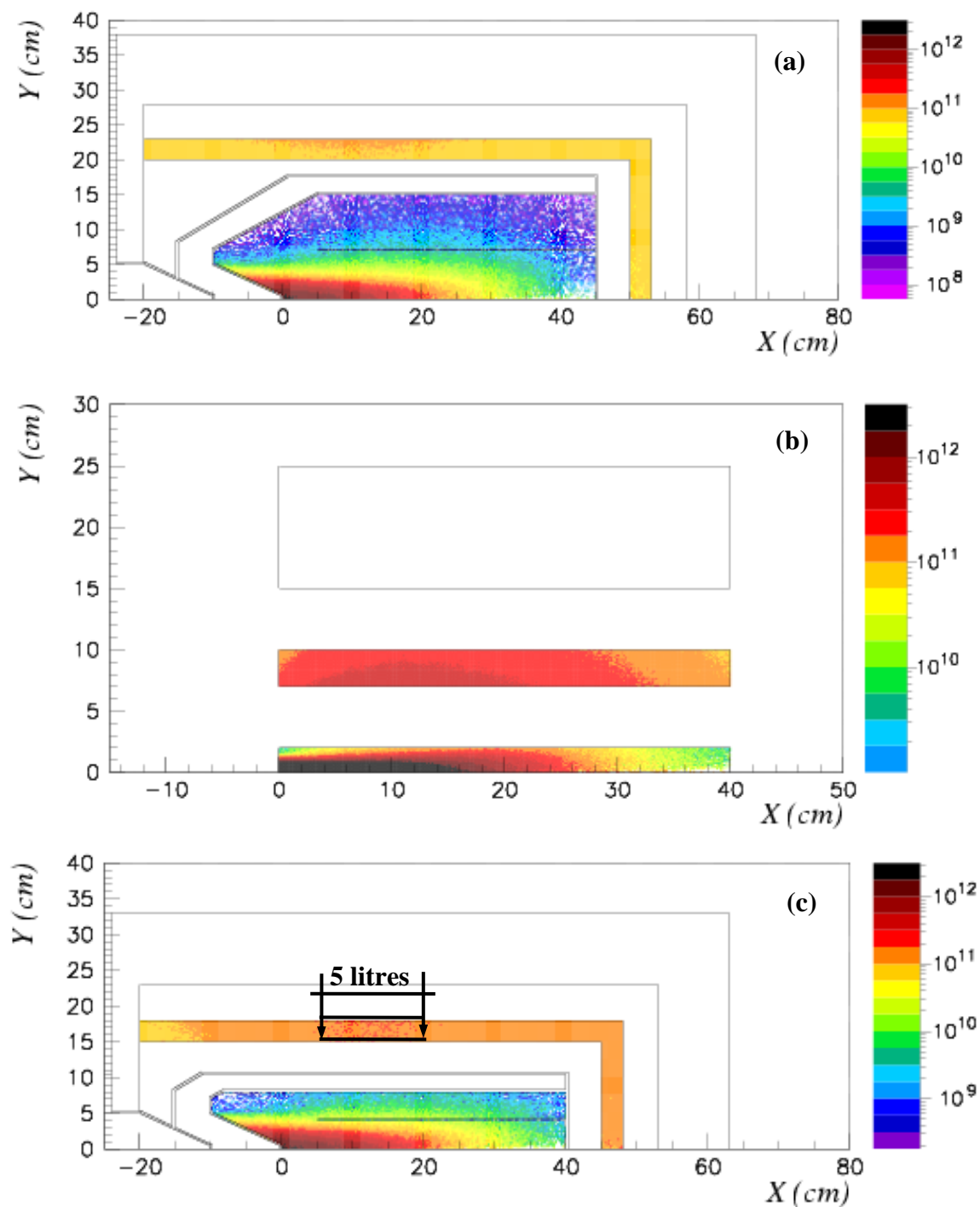


Figure 8. Fission density distribution ($\text{fissions}/\text{cm}^3/\text{s}/\text{MW}$ of beam) in (a) baseline configuration, (b) Hg-jet option and (c) scaled-down version.

Arguably, the most important design criteria are the production rates for the isotopes that are relevant for the experiment. An extensive list of those may be found in [6]. In this scope, Table 1 summarises the production rates for some of those isotopes (statistical errors below 5%) where the ratio between the baseline configuration rate and the other two cases is also shown. The Hg-jet option presents higher yields for all, ranging from 50% higher (^{90}Kr) to ~ 13 times higher (^{153}Sm).

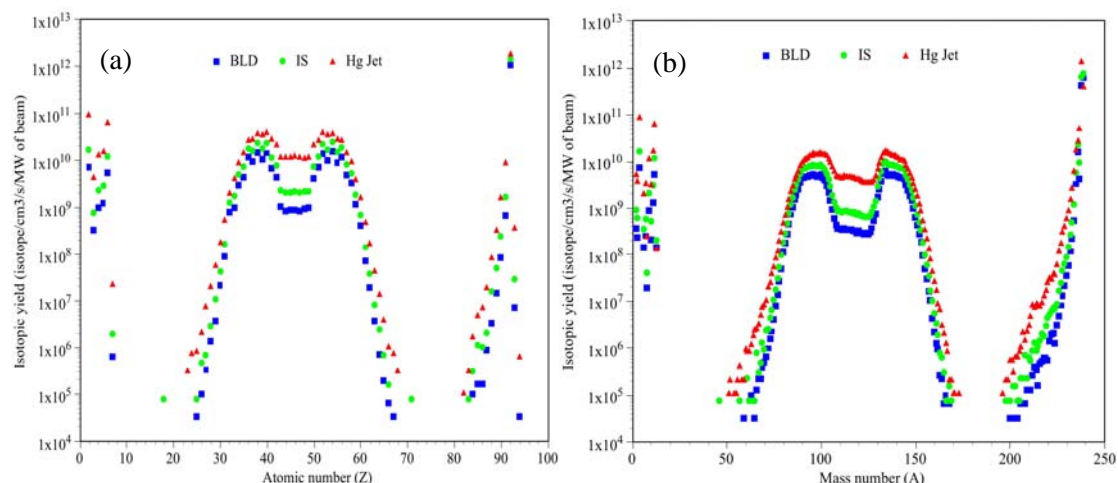


Figure 9. Fission yields (isotopes/cm³/s/MW of beam) in the three different configurations as a function of the atomic number Z (a), and the mass number A (b).

Table 1. Production rates (isotopes/cm³/s/MW of beam) for several relevant isotopes in the three Multi-MW target configurations analysed.

| (Z) Element-A | Baseline Conf. | Scaled-down Vers. | DV/BC | Hg jet | Hg-J/BC |
|---------------|----------------|-------------------|------------|---------|-------------|
| (31) Ga-81 | 1.4E+07 | 2.3E+07 | 1.6 | 7.7E+07 | 5.5 |
| (36) Kr-90 | 3.2E+09 | 4.7E+09 | 1.5 | 4.7E+09 | 1.5 |
| (38) Sr-89 | 1.4E+07 | 2.5E+07 | 1.8 | 1.2E+08 | 8.6 |
| (42) Mo-99 | 3.4E+07 | 6.2E+07 | 1.8 | 2.6E+08 | 7.6 |
| (50) Sn-132 | 6.4E+08 | 1.1E+09 | 1.7 | 1.9E+09 | 3.0 |
| (62) Sm-153 | 3.6E+05 | 8.4E+05 | 2.3 | 4.6E+06 | 12.7 |

The complete fission fragment distribution for all three target layouts, shown in Figure 10, may help to estimate the RIB production for every specific fission fragment. The yield values are given per cm³ per MW of beam power, and as a function of the atomic and mass numbers (Z and A, respectively). The stable isotopes are marked in black, allowing the distinction between neutron and proton-rich radioactive isotopes, on either side of the line of stability.

The standard fission target volumes being currently used at ISOLDE are ~ 30 cm³. Nevertheless, these assemblies could host much larger fission targets, increasing by at least two orders of magnitude (5 litre, Figure 8.c), consequently increasing by the same factor the fission yields, for the same proton current. Potentially these systems could include even larger targets, or a combination of different ones. This approach would entail very large RIB production gains, although extraction problems could be foreseen.

As mentioned before, the largest yield differences between targets occur in: (a) the fast-fission-induced symmetric fragments (central part of the colour plot), (b) multi-

fragmentation by-products (left-bottom and right-top edges of the plot) and (c) proton-rich isotopes (top region in the colour distribution).

The isotopes produced right along the edges of the colour plot present large statistical errors due to their low-production probability. Nevertheless, these plots appear as a good estimate of the distribution and magnitude for the fission fragments produced, at time=0, that is, before any radioactive decay or extraction losses.

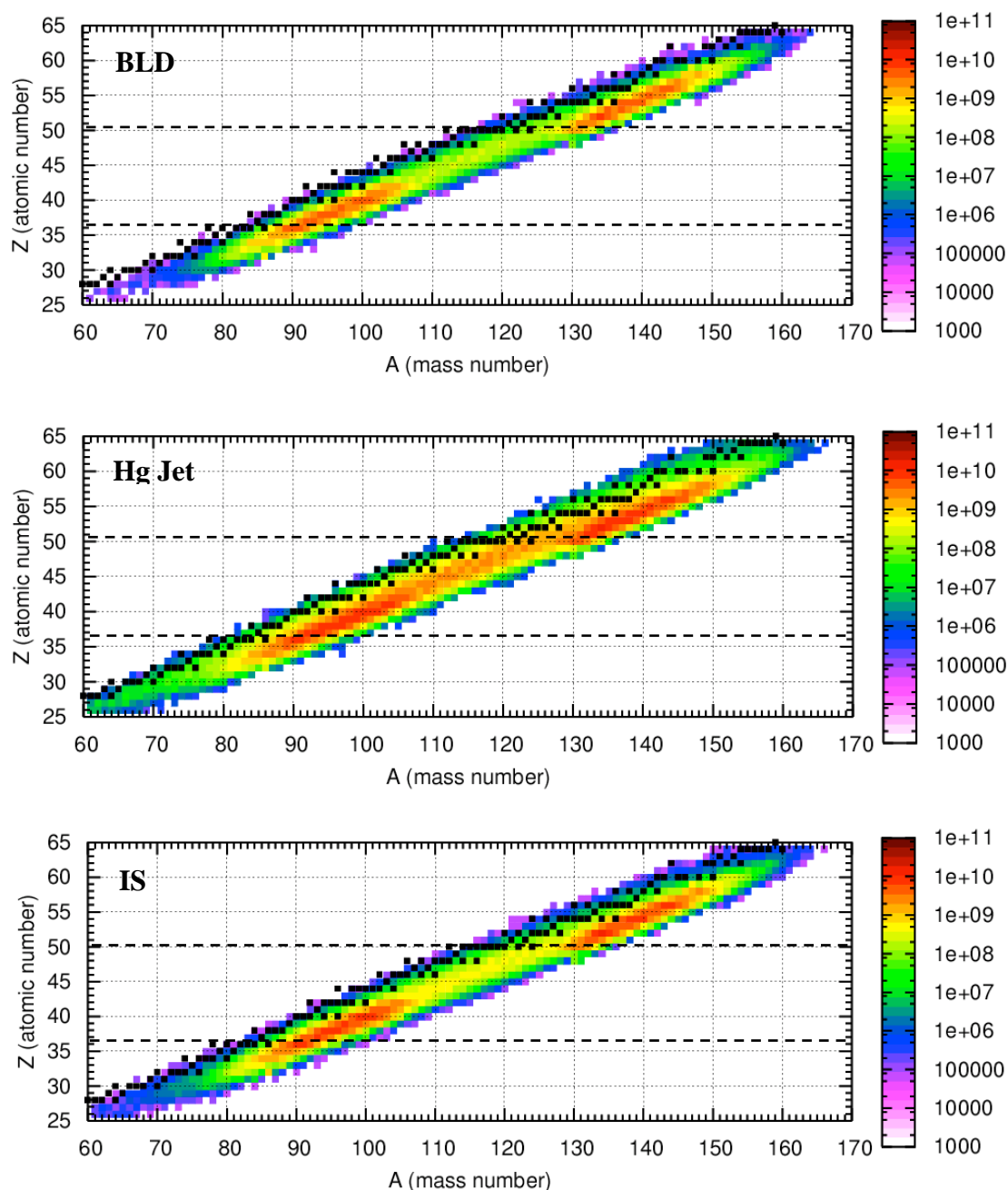


Figure 10. Quantitative fission fragment distribution for the three cases studied, the baseline configuration (BLD), its scale-down version (IS) and the Hg-jet option (Hg Jet).

As a matter of example, Figure 11 shows the distribution for the Kr (36) and Sn (50) isotopes, signalled by dashed lines in Figure 10, for the three studied target layouts. These elements are two of the most relevant ones for RIB production at EURISOL, as indicated in [6]. The differences in the yields between the three systems decrease as the number of neutrons increases. In other words, for these elements, neutron-rich isotopes are produced in increasingly similar quantities for all three scenarios.

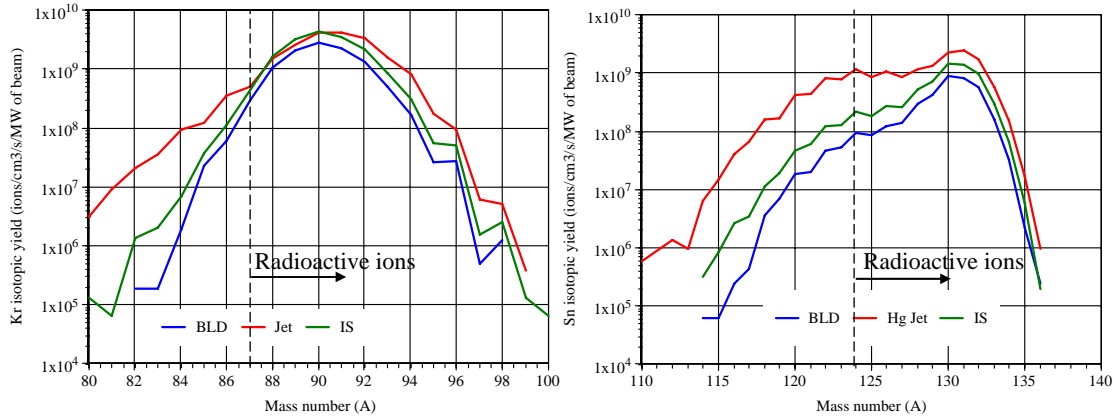


Figure 11. Isotopic yields for Kr and Sn, for the three target assemblies, baseline configuration (BLD), its scale-down version (IS) and the Hg-jet option (Hg Jet).

Integration of the Assemblies

The description of the integration parameters for the studied target layouts fall beyond the scope of this technical note, which is meant to compare the neutronic performance and RIB production capabilities of the assemblies.

For information on this matter, precise integration descriptions for the baseline configuration (which, in this scope, is identical to the scale-down version) and the Hg jet may be respectively found in [4] and [6].

Conclusions

A detailed comparison of performances between the baseline configuration, its scaled-down version and the Hg-jet option has been carried out, in the scope of the Multi-MW proton-to-neutron converter design.

The containment of the primary beam is successfully achieved by the baseline configuration, as suggested in [4]. The scaled-down version of this target allows some primary escapes, still three orders of magnitude below the escapes occurring in the

Hg-jet option. The latter would clearly require the use of a beam dump, with the subsequent misuse of a significant part of the proton beam.

The neutron flux is harder and more intense for the Hg jet, thus producing four times higher fission densities in the UCx target compared to the baseline configuration. The scaled-down version of the second achieves twice the fission densities of the baseline configuration. The largest differences occur in the symmetrical fission product yields, with up to one order of magnitude more high-energy fissions in the UCx target for the Hg jet compared to the baseline configuration (five times more compared to the scaled-down version of the baseline design).

This reflects in the production rates for specific isotopes, which range from 50% to 13 times higher yields for the Hg jet solution compared to the baseline configuration (from equal yields to 5.5 more yields compared to the scaled-down baseline version).

In terms of power densities, both the baseline configuration and its scaled-down version present values which appear to be technically acceptable [7], but which will require a specific cooling method for the beam window. In the case of the Hg jet, the very large power densities ($\sim 22 \text{ kW/cm}^3/\text{MW}$ of beam) would require very large flow rates, which would threaten the stability of the jet and are technologically challenging.

Therefore, the aimed fission product rates may be achievable with a compact Multi-MW target design of a proven kind with manageable power densities and homogeneous fission densities in the UCx target, which would improve the diffusion/effusion processes for the fission products.

Acknowledgements

We acknowledge the financial support of the European Commission under the 6th Framework Programme “Research Infrastructure Action- Structuring the European Research Area” EURISOL DS Project Contract no. 515768 RIDS. The EC is not liable for any use that may be made of the information contained herein.

References

- [1] “EURISOL DS; European Isotope Separation On-Line Radioactive Ion Beam Facility Design Study”, EC – FP6 Research Infrastructure Action- Structuring the European Research Area, Project Contract no. 515768 RIDS.
- [2] A. Fassò, A. Ferrari, J. Ranft, P.R. Sala, “FLUKA: Status and Prospective for Hadronic Applications”, , invited talk in the Proceedings of the MonteCarlo

- 2000 Conference, Lisbon, October 23--26 2000, A. Kling, F. Barao, M. Nakagawa, L. Tavora, P. Vaz eds., Springer-Verlag Berlin, p. 955-960, 2001. Also: “*Electron-photon transport in FLUKA: Status*”, A. Fassò, A. Ferrari, P.R. Sala, invited talk in the Proceedings of the MonteCarlo 2000 Conference, Lisbon, October 23--26 2000, A. Kling, F. Barao, M. Nakagawa, L. Tavora, P. Vaz eds., Springer-Verlag Berlin, p. 159-164, 2001.
- [3] A. Herrera-Matínez, Y. Kadi, “*Preliminary Study of the Liquid Metal Proton-to-Neutron Converter*”, EURISOL DS/TASK2/TN-05-01 and CERN-AB-2006-013 ATB Technical Note.
- [4] A. Herrera-Matínez, Y. Kadi, “*Neutronic Calculations for the Baseline Configuration of the Multi-MW Mercury Target*”, EURISOL DS/TASK2/TN-05-03 and CERN-AB ATB Technical Note.
- [5] L. Techio, “*Multi-MW Mercury Target Station Integration Studies*”, Topical meeting of the EURISOL-DS Management Board and Target Tasks, CERN, Switzerland, 10 November 2005.
- [6] J. Cornell (Ed.), “*The EURISOL Report; A Feasibility Study for a European Isotope-Separation-On-Line Radioactive Ion Beam Facility*”, GANIL, France, 2003.
- [7] Trevor Dury, “*First Thermal-Hydraulic Studies for the EURISOL High-Power Liquid-Metal Target, using Computational Fluid Dynamics*”, EURISOL DS/TASK2/TN-05-06 and PSI Report TM-42-05-47, December 2005.
- [8] R. Bennet et al., “*Studies of a Target System for a 4 MW, 24 GeV Proton Beam*”, A Proposal to the ISOLDE and Neutron Time-of-Flight Experiments Committee, CERN-INTC-2004-016, INTC-P-186, 26 April 2004.